The Vibrational Spectrum of the Neutral $(H_2O)_6$ Precursor to the "Magic" $(H_2O)_6^-$ Cluster Anion by Argon-Mediated, Population-Modulated Electron Attachment Spectroscopy

Eric G. Diken, William H. Robertson, and Mark A. Johnson*

Sterling Chemistry Laboratory, Yale University, P.O. Box 208107, New Haven, Connecticut 06520

Received: August 19, 2003

A new technique is introduced for the acquisition of size-selected neutral cluster spectra on the basis of argon-mediated, population-modulated electron attachment. This method is demonstrated and used to obtain the vibrational spectrum of the *neutral* water hexamer precursor to the $(H_2O)_6^-$ cluster ion. The mid-infrared spectrum of the neutral species is dominated by four intense features above 3400 cm^{-1}, clearly indicating that significant structural rearrangements occur upon slow electron attachment to form the "magic" hexamer cluster anion. Comparison with previous spectroscopic reports and theoretical predictions indicates that the low-energy "book" isomer is most consistent with the observed band pattern and is suggested to be the species that captures a low-energy electron to form the hexamer anion.

I. Introduction

Since the negatively charged water clusters, $(H_2O)_n^-$, were first observed by Haberland and co-workers in 1984,[1−3] these cluster analogues of the hydrated electron[4,5] have captured a great deal of interest from both theoretical and experimental groups.[6−27] Despite this intensive effort, however, there is no general agreement on the structures of the anions, and this uncertainty has frustrated attempts to explain the origin of the dramatic discontinuities observed in the $(H_2O)_n^-$ size distribution, where the $n = 2$, 6, and 7, and ≥ 11 clusters are much more abundant than their neighbors. Because the hexamer anion is the smallest cluster to display well-defined vibrational bands in the OH stretching region,[23] it has been subjected to particular scrutiny[6,12,23,28,29] with the goal of establishing the network morphologies of the two isomeric forms evident in its photoelectron spectrum.[3,22] Unfortunately, the vibrational band patterns are consistent with several of the locally stable minima calculated to exist on this complex potential energy landscape.[30] Candidate structures range from compact species such as the distorted prism isomer to an open, chainlike form.[12,20,31,32]

A key piece of missing information, which could shed light on the likely structures of the anions, is the mechanism by which the observed anions are created in the various ion sources. All such sources ultimately involve slow electron attachment[33,34] or Rydberg electron transfer[7,35] to neutral water clusters, but the structures of these particular clusters (that are susceptible to electron attachment) are presently unknown. In this paper, we address the anion formation mechanism by establishing the vibrational spectrum of the *neutral* hexamer precursor to the $(H_2O)_6^-$ cluster ion formed in a secondary electron attachment ion source.[36] To accomplish this, we introduce a method based on laser population labeling that exploits the unique opportunities afforded by argon-mediated "evaporative" electron attachment in supersonic jet sources:

$$(H_2O)_6{\cdot}Ar_m + e^- \rightarrow (H_2O)_6^-{\cdot}Ar_k + (m-k)Ar \qquad (1)$$

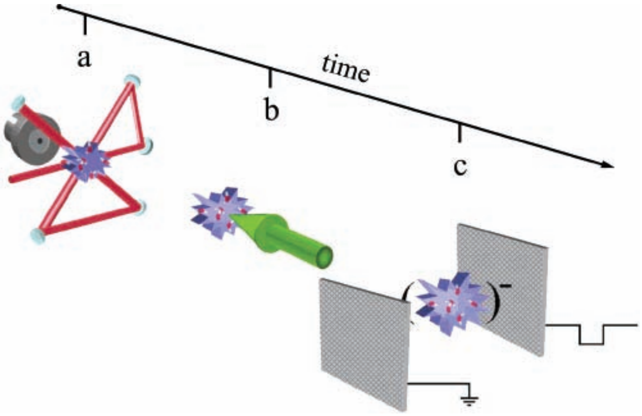

Figure 1. Schematic of the experimental arrangement and time sequence involving (a) multipassed, pulsed infrared (red beam) photoexcitation of the neutral cluster distribution, (b) delayed ionization via a pulsed 1 keV electron beam (depicted as a green arrow), and (c) creation of the anionic clusters by slow secondary electron attachment in the drift region between laser interaction and extraction into the time-of-flight mass spectrometer.

In eq 1, *m* indicates the number of argon atoms in the neutral cluster precursor leading to the observed anion with *k* argon atoms attached. The number of evaporated argon atoms reflects the energy release required to stabilize the nascent ion such that $m - k \sim \mathrm{AEA}/\Delta H_{\mathrm{evap}}$, where AEA is the adiabatic electron affinity of the hexamer and ΔH_{evap} is the heat of evaporation of argon atoms from the anionic cluster.

II. Experimental Section

IIA. Strategy. To acquire the spectrum of the $(H_2O)_6{\cdot}Ar_m$ neutral precursor in eq 1, we have modified our size-selected photofragmentation spectrometer[36] to allow infrared excitation in the source region as depicted in Figure 1. In this arrangement, we spatially (and temporally) separate the neutral cluster formation and electron attachment steps so as to allow laser excitation of the quiescent $(H_2O)_n{\cdot}Ar_m$ neutral distribution before the electrons are introduced. The laser crosses the unskimmed molecular beam about 2 cm downstream from the 0.5 mm diameter nozzle (i.e., 40 nozzle diameters) and is sufficiently

---

* To whom correspondence should be addressed

10.1021/jp0309973 CCC: $27.50

intense that excitation of a vibrational transition moves significant population in the neutral cluster distribution by argon predissociation:

$$(H_2O)_6{\cdot}Ar_p + h\nu \rightarrow (H_2O)_6{\cdot}Ar_l + (p - l)Ar \qquad (2)$$

Since photofragmentation reduces the number of argon atoms attached to a given water cluster (typically by six or seven in the mid-IR), infrared absorption also modulates the population of the argon-cluster precursor to the $(H_2O)_6^-{\cdot}Ar_k$ anion observed in the mass spectrum. By monitoring the intensity of a particular argon-solvated anion as the mid-IR laser is scanned through the OH stretching region, we can obtain the vibrational spectrum of its neutral precursor and thus characterize the network morphologies at play.

A key requirement for implementation of the method is that the population modulation step must occur in a regime where the density in the jet has dropped sufficiently to suppress collisions between the heavy particles (e.g., water and argon) and yet allow the very high cross-section (two-body) evaporative electron attachment events.[24] Under these conditions, retention of an argon atom in the product anion necessarily arises from a larger argon-solvated neutral, and because argon is much more weakly bound than a water molecule, the size of the core water cluster will be maintained. This method does not require photodestruction of the water cluster itself (like action spectroscopies carried out on the bare clusters)[37,38] and can be multiplexed in the sense that many neutral species can be obtained simultaneously with size-selectivity.

IIB. Technical Details. In our apparatus, the laser-modulated neutral clusters are converted to negative ions by introducing a pulsed 1 keV electron beam, counterpropagating with the neutral expansion, approximately 1 μs after the laser pulse. This generates slow secondary electrons all along the axis of the supersonic flow, creating a neutral plasma whose density falls off rapidly away from the nozzle. Negative ions are formed throughout the entire expansion, but it is possible to isolate only those ions formed from neutrals that interacted with the laser by carefully controlling the time between the laser pulse and the draw-out high-voltage pulse injecting the ions into a transverse time-of-flight mass spectrometer. The distance between the laser interaction region and the entrance to the mass spectrometer is 15 cm, and the velocity of all the species in the expansion are sharply centered around $v_o \sim 4 \times 10^4$ cm/s. Thus, the laser-induced population modulation results in a local "hole" (or enhancement) in neutral density that arrives at the TOF aperture about 375 μs after the laser pulse.

While electron attachment in the low-density environment of the expansion (i.e., beyond the laser region) is much less efficient than near the nozzle, the long interaction time allows for sufficient negative ion formation to readily observe the cluster anion distribution. The evaporative electron attachment dynamics (eq 1) do not significantly change the laboratory velocities of the clusters. Interestingly, the anionic cluster distribution formed by attachment late in the expansion (as opposed to our usual approach of electron attachment in the high-density region at the orifice) gives rise to less intensity as expected, but the cluster distribution peaks with a much larger number of attached argon atoms.

Infrared radiation is obtained from a Nd:YAG pumped, KTP-based (*LaserVision*) optical parametric oscillator which generates approximately 5 mJ/pulse in the 3−4 μm region by parametric amplification with the Nd:YAG fundamental (1064 nm). The bandwidth of the infrared beam is approximately 2 cm^{-1}. Each reported spectrum has been corrected for laser power fluctuations over the spectral range and is the accumulation of 30−40 individual scans. The maximum observed modulations are about 30%.

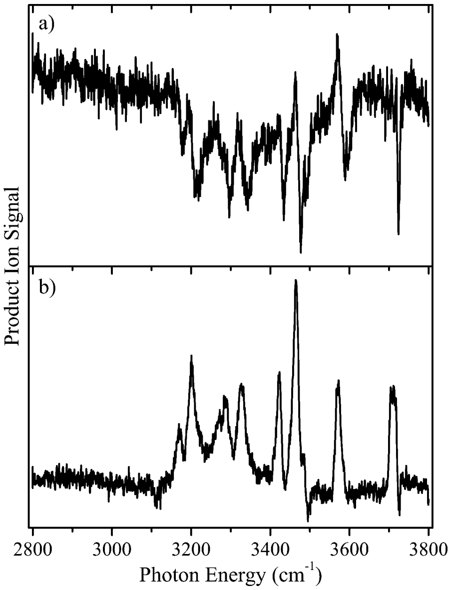

Figure 2. Argon-mediated, population-modulated electron attachment mid-IR spectra of the neutral water hexamer obtained by monitoring the mass-selected, anionic product after slow electron attachment. The spectrum in a is obtained when monitoring modulation of $(H_2O)_6^-{\cdot}Ar_1$, while b is generated by detection of $(H_2O)_6^-$. Note that the spectrum in b maintains the signature infrared spectrum obtained in the argon-solvated cluster, but the features appear preferentially in an ion-enhancement mode.

III. Results and Discussion

Figure 2a displays the spectrum of the neutral water hexamer leading to production of the $(H_2O)_6^-{\cdot}Ar$ anion cluster. This spectrum displays a sharp, downward-going band at the position of the free OH stretch (3711 cm^{-1}) and a series of broader bands extending down to 3100 cm^{-1}. We have also obtained the spectrum of the precursor to the heptamer anion, and that species displays a dramatically different spectrum than is obtained when isolating $(H_2O)_6^-{\cdot}Ar$, thus establishing that this method indeed overcomes complications from cascade processes within the $(H_2O)_n$ manifold.

The features around 3572 and 3464 cm^{-1} in Figure 2a are curious in that they appear with asymmetric, derivative-looking line shapes. This asymmetry is such that the low-energy sides of the bands display an enhancement of ion yield while the high-energy sides correspond to ion depletion. This behavior is readily understood in the context of the two photochemical routes which lead to population labeling of the $(H_2O)_6{\cdot}Ar_m$ neutral precursor to the observed $(H_2O)_6^-{\cdot}Ar$ anion:

$$(H_2O)_6{\cdot}Ar_p + h\nu \rightarrow (H_2O)_6{\cdot}Ar_m + (p - m)Ar \qquad (3a)$$

$$(H_2O)_6{\cdot}Ar_m + h\nu \rightarrow (H_2O)_6 + mAr \qquad (3b)$$

$$(H_2O)_6{\cdot}Ar_m + e^- \rightarrow (H_2O)_6^-{\cdot}Ar + (m - p)Ar \qquad (3c)$$

Since there are both production (eq 3a) and removal (eq 3b) pathways involving $(H_2O)_6{\cdot}Ar_m$, the net anion population modulation (eq 3c) depends on the relative initial populations of the clusters with p and m argon atoms, respectively, and their (argon-size-dependent) absorption cross sections at a particular excitation wavelength. Huisken and co-workers[37] have shown that, in the neutral water dimer, attachment of argon atoms leads to a red-shift in the H-bonded OH stretching mode, with large Ar clusters yielding an asymptotic shift of about 25 cm^{-1} relative to the transition in the isolated dimer. With this in mind, the "derivative" line shapes can be explained as a consequence of the larger argon clusters absorbing to the red of smaller clusters. Selective excitation of larger clusters on the red side of the band would give rise to enhancement via eq 3a, while tuning toward the isolated band origin on the blue side excites smaller clusters which lead to depletion via eq 3b. Since about six argon atoms should be ejected upon excitation in the OH stretching region,[39] the displacement between the two out-of-phase intensity modulations would indicate a sequential argon shift of about 2 cm^{-1}/Ar for the 3572 cm^{-1} band. This value is in line with previously observed shifts,[39−41] and the vibrational mode specificity of the argon matrix shift[42] would explain why some bands are more susceptible to the effect than others.

In light of the above discussion, derivative-type line shapes appear intrinsic to this method. However, we have observed an interesting and unexpected simplicity in the spectra when we monitor production of the bare $(H_2O)_6^-$ ion in a regime where we tune the source conditions to optimize very large argon clusters in the product $(H_2O)_6^-{\cdot}Ar_k$ anions. This spectrum is presented in Figure 2b and displays the same bands observed when monitoring production of $(H_2O)_6^-{\cdot}Ar$, and most importantly, contains no extra features. These band profiles occur almost exclusively as positive features (corresponding to ion signal enhancements), and all the observed bands are found slightly to the red of the negative-going peaks in the $(H_2O)_6^-{\cdot}Ar$ spectrum (Figure 2a).

The red-shift in the bands obtained by monitoring the bare hexamer ion (Figure 2b) establishes that they arise from larger argon clusters than those detected through negative modulations of the $(H_2O)_6^-{\cdot}Ar$ ion. The overwhelmingly positive peaks (rather than derivative line shapes) dictate that more absorption events lead to enhancement of anion precursors than to their destruction. One clue to the cause of this behavior is that it occurs under conditions where the $(H_2O)_6^-{\cdot}Ar_k$ cluster ion distribution is inverted (in the sense that there is more population at the larger sizes) with an intensity maximum in the range $k = 5-7$.[23] In this context, we can understand the dominance of the enhancement pathway by considering the sequential multiphoton absorption processes in the large argon clusters, which very likely occur in the high-fluence, multipassed arrangement used for neutral excitation (step a in Figure 1). We expect the stepwise shift in the OH stretching bands to be greatest for addition of the first few argon atoms, with the larger clusters asymptotically approaching the matrix value. Thus, the large clusters should be able to undergo several absorption/evaporation cycles in the 8 ns pulse length and 2 cm^{-1} bandwidth of the laser, each time shedding six or so argon atoms. This process will continue until the smaller fragments eventually tune out of resonance with the laser, effectively redistributing the upper range of the argon cluster distribution to the smaller sizes which yield enhancement of anion production. All neutral $(H_2O)_6{\cdot}Ar_m$ clusters with $1 \le m \le (AEA/\Delta H_{evap})$ yield such enhancements of the bare ion, effectively integrating the effect, while only the neutral with $m \sim 1 + (AEA/\Delta H_{evap})$ contributes to $(H_2O)_6^-{\cdot}Ar$ formation. These considerations also serve to expose some of the complexities inherent in the method, where the observed signals may well depend on the magnitudes of the argon-induced band shifts and the adiabatic electron affinities (AEAs) of the product anions.

TABLE 1: Calculated and Experimental (±5 cm^{-1}) Vibrational Transition Energies for the Neutral Water Hexamer

this work[a]	$C_6H_6{\cdot}(H_2O)_6$ [b]	book[c]	cage[c]	ring[c]
3169	3078		3157	
3201	3210	3218	3352	
3287	3308	3281	3392	
3327	3389	3331	3422	3318 (×2)
3423	3408	3413	3490	3389
3464	3453	3457	3546	
	3508	3480	3593	
3572	3578	3602	3628	
	3636[d]			
	3708	3704	3706	
3711	3714	3715	3711	3716
		3718	3715	3717 (×2)
		3721 (×2)	3724	

[a] Estimated uncertainty (±5 cm^{-1}). [b] Extracted from ref 46. [c] Extracted from ref 49 by scaling with a value of 0.94 to account for anharmonicity by normalization to the symmetric and asymmetric stretches for the isolated water monomer. [d] π-H-bond to benzene ring.

To test the hypothesis that large argon clusters are causing the positive modulations observed in Figure 2b, we have also acquired spectra by monitoring the bare hexamer anion under conditions where so few argon atoms are attached that it is unlikely for the neutral argon distribution to be inverted. In this regime, the resulting spectrum is indeed observed to be negative-going, with blue-shifted features relative to those in Figure 2b. It is important to emphasize that even in this very different configuration, no new bands are observed and again there is no contamination arising from excitation of the $(H_2O)_7$ cluster. The observed bands of the neutral hexamer prepared in this study are collected in Table 1.

It might, at first, be surprising that modulation of the bare ion is not contaminated by photoexcitation of larger or smaller water clusters. It is likely that this favorable scenario results from a somewhat special circumstance involving the size-dependent decay pathways of warm water clusters. Previous studies[43−45] have established that, below $n = 15$, both condensation and evaporation of water molecules, which could change the shape of a nascent $(H_2O)_n^-$ distribution, are suppressed because the electron evaporation channel lies below the energy required to dissociate a water molecule. Thus, the evaporative attachment mechanism involving a water molecule:

$$(H_2O)_n + e^- \rightarrow (H_2O)_{n-1}^- + H_2O \tag{4}$$

is much less efficient that the analogue involving evaporation of a weakly bound argon atom (eq 1). Thus, the observed bare $(H_2O)_n^-$ species are very likely created from argon-solvated neutrals, and their response to population modulation is not contaminated by cascade processes (which must be present) in the manifold of bare neutral water clusters.

Having established that the observed spectral features are indeed due to the neutral water hexamer, it is of interest to compare this spectrum with the vibrational band patterns previously reported[46−49] for $(H_2O)_6$. The most definitive immediate conclusion is the isomer leading to the anion is not (at least predominantly) the cyclic form, as this species should have a very simple spectrum (see Table 1, labeled "ring"), with two strongly red-shifted features and a sharp free OH feature near 3700 cm^{-1}.[49] We indeed observe a prominent free OH band at 3711 cm^{-1} but also a series of intense bands throughout the spectrum. Unfortunately, there are no complete spectra of the *isolated* hexamer neutral for comparison. The cyclic isomer has only been generated in condensed media, but because of the congestion presented by the smaller clusters, only one of its bands has been assigned (3335 cm^{-1} in liquid He droplets[47] and 3319 cm^{-1} in solid pH_2 [48]). In free jets, ring-down methods[50,51] have been effective but are also not size-selective. There is one size-selective spectroscopic technique developed by the Gottingen group,[37,38] on the basis of inelastic helium scattering, which has been used extensively on the small water clusters. Unfortunately, the hexamer appears to present complications as both larger and smaller clusters have been published and analyzed, while the hexamer is yet to be reported.

For comparison, we have therefore included the bands observed by Zwier and co-workers[46] in Table 1, who reported the spectrum of $(H_2O)_6$ attached to a benzene molecule using the RIDIRS technique. Two of these features above 3400 cm^{-1} are in remarkable agreement with the anion modulation spectrum, with the only missing band being the π-H-bonded OH stretch at 3636 cm^{-1}, which obviously should be missing in the argon-solvated hexamer. This leaves open the question of whether the differences between the spectra recorded by anion-population modulation and RIDIRS are due to the benzene perturbation, or in fact reflect a different isomeric form of the hexamer.

While the structural assignment of the anionic hexamer by comparison with calculated band patterns has proven difficult because of the complexities introduced by the diffuse excess electron, the neutral species might be expected to be more straightforward, and we include very recent calculations of fundamentals for the lowest energy structures, the cage, book, and ring forms, in Table 1. Interestingly, there is much better agreement with the book form rather than the cage, even though the cage has been suggested[30,52] to be the likely isomer created in jet sources on the basis of theory. The major differences between the calculated and observed bands occur in the region around 3250 cm^{-1}, where we expect strong interactions between the OH stretches and the H_2O intramolecular bending vibrations.[53,54] Obviously, it is possible that several isomers could be present, but the band pattern is not dependent on the number of attached argon atoms, which might be expected to affect the relative abundance of two nearly isoenergetic isomers.[55] This indicates that the observed spectrum most likely results from a single isomer.

It is also of interest to compare the spectrum of the neutral precursor with the spectrum of the $(H_2O)_6^-$ product ion, reported several years ago.[23] This comparison is presented in Figure 3, with the argon predissociation spectrum of $(H_2O)_6^-{\cdot}Ar_7$ reproduced in the upper trace and the $(H_2O)_6$ spectrum obtained here displayed in the lower trace. The features in both spectra span a similar energy range, but the patterns are completely different, indicating that a substantial change in morphology occurs upon electron attachment. First, the prominent free OH band around 3700 cm^{-1} is absent in the anion, where a doublet appears about 50 cm^{-1} below the free OH. Second, the intensity profiles are dramatically changed upon electron attachment. The spectrum of the anion is dominated by the very strong doublet around 3300 cm^{-1}, while the most intense feature in the neutral spectrum appears around 3450 cm^{-1} and the bands appear with a more even distribution of oscillator strength. Another qualitative aspect of the spectral changes is that the neutral spectrum extends farther to the red than does that of the ion. This is an unusual scenario, as the introduction of an excess charge typically results in enhanced red-shifts in charge-localized systems.[56−59] With high signal-to-noise spectra of this isolated hexamer in hand, it will be valuable to revisit this species with the most advanced theoretical methods to better define the isomer at play.

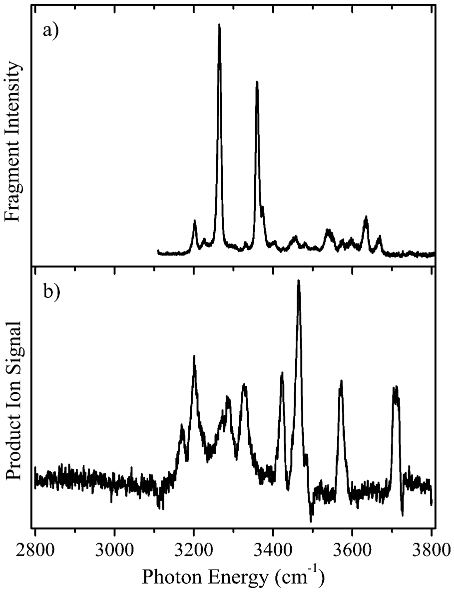

Figure 3. Comparison between vibrational predissociation spectra of (a) $(H_2O)_6^-{\cdot}Ar_7$, reproduced from ref 23, and (b) the neutral $(H_2O)_6$ complex, obtained by argon-mediated, population-modulated electron attachment spectroscopy (this work).

IV. Conclusions

Summarizing, we have demonstrated a new technique for obtaining size-selective spectra of neutral clusters on the basis of argon-mediated, population-modulated electron attachment and have applied it to the case of the water hexamer. The resulting spectra are quite different than the band pattern found in the hexamer anion, indicating significant rearrangement upon electron attachment. This technique is well suited to study many types of neutral species, and we are presently engaged in extending this work to study the dissolution of an acid molecule in small water clusters.[60,61] In this class of neutral clusters, the slow electrons should selectively attach to the strong dipole moment associated with the dissociated, zwitter ionic forms.

Acknowledgment. We thank the U.S. Department of Energy under grant DR-FG02-00ER15066 for support of this work. M.A.J. also acknowledges influential conversations with Profs. J. P. Schermann and C. Desfrancois in laying out the basic strategy of similar experiments involving Rydberg electron transfer and with Prof. K. D. Jordan regarding the structural implications of the spectra. We also acknowledge Prof. U. Buck for sharing unpublished results on the water hexamer spectrum.

References and Notes

(1) Haberland, H.; Schindler, H.-G.; Worsnop, D. R. *Ber. Bunsen-Ges. Phys. Chem.* **1984**, *88*, 271.

(2) Haberland, H.; Langosh, H.; Schindler, H.-G.; Worsnop, D. R. *J. Phys. Chem.* **1984**, *88*, 3903.

(3) Coe, J. V.; Lee, G. H.; Eaton, J. G.; Arnold, S. T.; Sarkas, H. W.; Bowen, K. H.; Ludewigt, C.; Haberland, H.; Worsnop, D. R. *J. Chem. Phys.* **1990**, *92*, 3980.

(4) Hart, E. J.; Boag, J. W. *J. Am. Chem. Soc.* **1962**, *84*, 4090.

(5) Keene, J. P. *Nature* **1963**, *197*, 47.

(6) Lee, G. H.; Arnold, S. T.; Eaton, J. G.; Sarkas, H. W.; Bowen, K. H.; Ludewigt, C.; Haberland, H. *Z. Phys. D* **1991**, *20*, 9.

(7) Desfrancois, C.; Khelifa, N.; Lisfi, A.; Schermann, J. P.; Eaton, J. G.; Bowen, K. H. *J. Chem. Phys.* **1991**, *95*, 7760.

(8) Misaizu, F.; Kondow, T.; Kuchitsu, K. *Chem. Phys. Lett.* **1991**, *178*, 369.

(9) Bartels, D. M. *J. Chem. Phys.* **2001**, *115*, 4404.

(10) Smith, D. M. A.; Smets, J.; Elkadi, Y.; Adamowicz, L. *J. Chem. Phys.* **1997**, *107*, 5788.

(11) Tsurusawa, T.; Iwata, S. *Chem. Phys. Lett.* **1998**, *287*, 553.

(12) Kim, K. S.; Park, I.; Lee, S.; Cho, K.; Lee, J. Y.; Kim, J.; Joannopoulos, J. D. *Phys. Rev. Lett.* **1996**, *76*, 956.

(13) Kim, K. S.; Lee, S.; Kim, J.; Lee, J. Y. *J. Am. Chem. Soc.* **1997**, *119*, 9329.

(14) Lee, S.; Lee, S. J.; Lee, J. Y.; Kim, J.; Kim, K. S.; Park, I.; Cho, K.; Joannopoulos, J. D. *Chem. Phys. Lett.* **1996**, *254*, 128.

(15) Barnett, R. N.; Landman, U.; Cleveland, C. L.; Jortner, J. *J. Chem. Phys.* **1988**, *88*, 4421.

(16) Barnett, R. N.; Landman, U.; Cleveland, C. L.; Jortner, J. *J. Chem. Phys.* **1988**, *88*, 4429.

(17) Novakovskaya, Y. V.; Stepanov, N. F. *Int. J. Quantum Chem.* **1997**, *63*, 737.

(18) Bar-on, A.; Naaman, R. *J. Chem. Phys.* **1989**, *90*, 5198.

(19) Wang, F.; Jordan, K. D. *J. Chem. Phys.* **2002**, *116*, 6973.

(20) Ayotte, P.; Weddle, G. H.; Bailey, C. G.; Johnson, M. A.; Vila, F.; Jordan, K. D. *J. Chem. Phys.* **1999**, *110*, 6268.

(21) Kelley, J. A.; Weddle, G. H.; Robertson, W. H.; Johnson, M. A. *J. Chem. Phys.* **2002**, *116*, 1201.

(22) Bailey, C. G.; Kim, J.; Johnson, M. A. *J. Phys. Chem.* **1996**, *100*, 16782.

(23) Ayotte, P.; Bailey, C. G.; Kim, J.; Johnson, M. A. *J. Chem. Phys.* **1998**, *108*, 444.

(24) Weber, J. M.; Leber, E.; Ruf, M. W.; Hotop, H. *Eur. Phys. J.* **1999**, *7*, 587.

(25) Khan, A. *J. Chem. Phys.* **2003**, *118*, 1684.

(26) Beyer, M. K.; Fox, B. S.; Reinhard, B. M.; Bondybey, V. E. *J. Chem. Phys.* **2001**, *115*, 9288.

(27) Lee, H. M.; Lee, S.; Kim, K. S. *J. Chem. Phys.* **2003**, *119*, 187.

(28) Lee, H. M.; Suh, S. B.; Kim, K. S. *Bull. Korean Chem. Soc.* **2000**, *21*, 555.

(29) Bailey, C. G.; Johnson, M. A. *Chem. Phys. Lett.* **1997**, *265*, 185.

(30) Tsai, C. J.; Jordan, K. D. *Chem. Phys. Lett.* **1993**, *213*, 181.

(31) Tsurusawa, T.; Iwata, S. *Chem. Phys. Lett.* **1999**, *315*, 433.

(32) Suh, S. B.; Lee, H. M.; Kim, J.; Lee, J. Y.; Kim, K. S. *J. Chem. Phys.* **2000**, *113*, 5273.

(33) Knapp, M.; Echt, O.; Kreisle, D.; Recknagel, E. *J. Phys. Chem.* **1987**, *91*, 2601.

(34) Stamatovic, A.; Leiter, K.; Ritter, W.; Stephan, K.; Mark, T. D. *J. Chem. Phys.* **1985**, *83*, 2942.

(35) Stockdale, J. A.; Davis, F. J.; Compton, R. N.; Klots, C. E. *J. Chem. Phys.* **1973**, *60*, 4279.

(36) Johnson, M. A.; Lineberger, W. C. *Techniques for the Study of Gas-Phase Ion Molecule Reactions*. Wiley: New York, 1988; p 591.

(37) Buck, U.; Huisken, F. *Chem. Rev.* **2000**, *100*, 3863.

(38) Buck, U.; Ettischer, I.; Melzer, M.; Buch, V.; Sadlej, J. *Phys. Rev. Lett.* **1998**, *80*, 2578.

(39) Ayotte, P.; Weddle, G. H.; Kim, J.; Johnson, M. A. *Chem. Phys.* **1998**, *239*, 485.

(40) Kelley, J. A.; Weber, J. M.; Lisle, K. M.; Robertson, W. H.; Ayotte, P.; Johnson, M. A. *Chem. Phys. Lett.* **2000**, *327*, 1.

(41) Corcelli, S. A.; Kelley, J. A.; Tully, J. C.; Johnson, M. A. *J. Phys. Chem.* **2002**, *106*, 4872.

(42) Forney, D.; Jacox, M. E.; Thompson, W. E. *J. Mol. Spectrosc.* **1993**, *157*, 479.

(43) Campagnola, P. J.; Cyr, D. M.; Johnson, M. A. *Chem. Phys. Lett.* **1991**, *181*, 206.

(44) Posey, L. A.; Johnson, M. A. *J. Chem. Phys.* **1988**, *89*, 4807.

(45) Posey, L. A.; Campagnola, P. J.; Johnson, M. A.; Lee, G. H.; Eaton, J. G.; Bowen, K. H. J. *J. Chem. Phys.* **1989**, *91*, 6536.

(46) Pribble, R. N.; Zwier, T. S. *Science* **1994**, *265*, 75.

(47) Nauta, K.; Miller, R. E. *Science* **2000**, *287*, 293.

(48) Fajardo, M. E.; Tam, S. *J. Chem. Phys.* **2001**, *115*, 6807.

(49) Kim, J.; Kim, K. S. *J. Chem. Phys.* **1998**, *109*, 5886.

(50) Paul, J. B.; Provencal, R. A.; Chapo, C.; Petterson, A.; Saykally, R. J. *J. Chem. Phys.* **1998**, *109*, 10201.

(51) Paul, J. B.; Provencal, R. A.; Chapo, C.; Roth, K.; Casaes, R.; Saykally, R. J. *J. Phys. Chem.* **1999**, *103*, 2972.

(52) Kim, K.; Jordan, K. D.; Zwier, T. S. *J. Am. Chem. Soc.* **1994**, *116*, 11568.

(53) Ayotte, P.; Weddle, G. H.; Kim, J.; Johnson, M. A. *J. Am. Chem. Soc.* **1998**, *120*, 12361.

(54) Robertson, W. H.; Weddle, G. H.; Kelley, J. A.; Johnson, M. A. *J. Phys. Chem. A* **2002**, *106*, 1205.

(55) Kim, J.; Becker, I.; Cheshnovsky, O.; Johnson, M. A. *Chem. Phys. Lett.* **1998**, *297*, 90.

(56) Ayotte, P.; Weddle, G. H.; Kim, J.; Kelley, J. A.; Johnson, M. A. *J. Phys. Chem. A* **1999**, *103*, 443.

(57) Ayotte, P.; Weddle, G. H.; Johnson, M. A. *J. Chem. Phys.* **1999**, *110*, 7129.

(58) Ayotte, P.; Nielsen, S. B.; Weddle, G. H.; Johnson, M. A.; Xantheas, S. S. *J. Phys. Chem. A* **1999**, *103*, 10665.

(59) Robertson, W. H.; Diken, E. G.; Price, E. A.; Shin, J.-W.; Johnson, M. A. *Science* **2003**, *299*, 1367.

(60) Hurley, S. M.; Dermota, T. E.; Hydutsky, D. P.; Castleman, A. W., Jr. *Science* **2002**, *298*, 202.

(61) Robertson, W. H.; Johnson, M. A. *Science* **2002**, *298*, 69.